On the internal structure of Black Holes

Farid Abrari
1400 Woodeden Dr, Mississauga, Ont, L5H 2T9, Canada
farid.abrari@gmail.com
https://orcid.org/0000-0003-1062-0732

November 4, 2025

Abstract

The combined theory of Special Relativity and Quantum Mechanics (c-SRQM) suggests the existence of a *Primordial Stem Particle* (PSP) whose rest mass $\bar{m}$ is thought to be the cutoff limit for massless particles. At its condensed state of various quantum energy levels, the PSP is thought to be the sole constituent of black holes singularity, and in its free state, the PSP is thought to permeate the entire universe as a relic left from the Big Bang. The c-SRQM theory also suggests a physical limit $a_u = c^2/A$ for acceleration, and with that, arrives at the concept of the Unit Black Hole (UBH) with mass $M_1 = Ac^2/4G$ whose gravitational pull at the event horizon of diameter A is equal to a_u. The PSP constituents of a stand-alone UBH have the spatial uncertainty $\delta x = A$, thereby confining the particles to the very surface of the UBH event horizon. For larger black holes with index $b > 1$ and mass $M_b > M_1$, a layered internal structure emerges comprising of b concentric spherical shells. The quantum index of constituents of each shell matches their shell number: the innermost shell 1, ie. UBH, is occupied by the PSPs at quantum energy level $n = 1$, the following shell 2 is occupied by the PSPs at quantum energy level $n = 2$, and so on until the outermost shell b which is occupied by the PSPs at quantum energy level $n = b$. These concentric spherical shells create the *core* or the *physical singularity* of black holes, a structure somewhat similar to but far simpler than the electron shells in the atomic structure of ordinary matter. A set of LIGO-Virgo Gravitational Wave data is used to constrain the UBH mass median to 7.402E23 (kg) and its core diameter to 2.197 (mm). The resulting PSP mass is constrained to a median of 1.006E-39 (kg).

1 Combined theory of SR and QM

We will start the article with a review the essential aspects of the c-SRQM first. Then will show how the findings from the theory can be used to gain insight on the internal structure of the black holes singularity and their composition. For that, consider a particle with mass m and its nearest [1] frame $I(x, t)$, moving undisturbed [2] in vacuum on a rectilinear path under

[1] In the c-SRQM theory, the notion of rest frame of SR is revised to: *an inertial frame wherein the uncertainty in position and momentum of a quantum particle is at a minimum.* The rest frame in the combined theory is therefore named as the *nearest* frame - on the basis that the particle is at the closest state to being stationary in that frame. The word nearest might also be useful to remind the words *near* and *rest.*

[2] Implying the particle trajectory or momentum is not influenced by any external factors, such as gravity, radiation or interaction with other particles.

a constant momentum p'. The particle is assumed to be in a non-stationary state along the x'-axis of another inertial frame of reference, $I'(x', t')$. To limit ourselves to one a dimensional analysis, we further assume the spatial axes x and x' of the frames I and I' are parallel.

From SR, the spacetime coordinates of any *event* registered in these two inertial frames of reference, I and I', are related to each other through the Lorentz transformation [1]. One such event is when the origins of the frames of reference I and I' are both *simultaneous* and *coincident*. As shown in the Lorentz diagram, Fig 1, the spacetime coordinate of this event is marked by the event E_0 where the spatial and time coordinates of both frames are set at zero, hence, meeting the simultaneity and coincidence condition of the event. Now consider

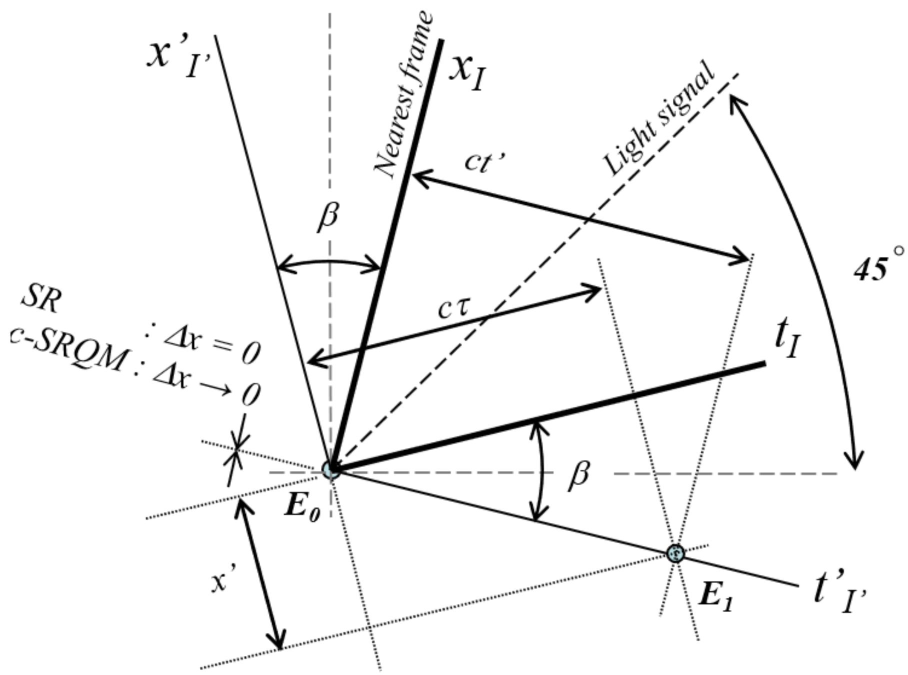

Figure 1: Lorentz diagram between two inertial frames of reference I and I'

another event when the particle is at a distance x' from the origin of I', when the coordinate clock in I' reads time t'. This corresponds to the coordinate clock in the nearest frame I reading the particle's *proper time* τ. The spacetime coordinate of that event is marked by the event E_1 in Fig 1. The *spatial distance* between the events E_0 and E_1 in the frame I' is $\Delta x' = x'$; while in the particle's nearest frame I, the distance between the events is $\Delta x \to 0$. Note that in SR, $\Delta x = 0$ precisely, as there is no uncertainty associated with the position of a particle in its rest frame. In the c-SRQM theory, however, there is uncertainty in the position of a particle even in its nearest frame. As we will discuss shortly, the spatial uncertainty in the nearest frame is found to be a function of the particle mass such that the higher the mass, the lower the spatial uncertainty. The angle β between the inertial frames of reference I and I' is given by $\sin(\beta) = v'/c = x'/ct'$, where c is the speed of light in vacuum. From the relationship, it is evident that as $v' \to c$ the angle $\beta \to \pi/2$. At the other extreme, when the objects are relatively stationary to each other, i.e. as $v' \to 0$ the angle $\beta \to 0$, which results in the coordinate frames overlapping each other. Since SR is a *deterministic* theory, there are no uncertainties $(\delta x', c\delta t')$ associated with the spacetime coordinate (x', ct') of the event E_1. Moreover, being a *continuous* theory, the particle velocity v' or its momentum p' are continuous variables. In the following sections, the quantum uncertainties are introduced in the context of Special Relativity.

2 Quantum Wavefunction

Limiting ourselves to a special case in which the particle's momentum is constant, next we define the wavefunction $\psi(x)$ of the particle of mass m such that the square of its magnitude $|\psi(x)|^2$ to have the following character:

$$|\psi(x')|^2 = \begin{cases} 1/\epsilon & |x'| < \epsilon/2 \\ 0 & \text{otherwise} \end{cases} \tag{1}$$

By definition, the function $|\psi(x')|^2$ could be interpreted as the *probability density distribution* of the particle's position along x'-axis. The dimensionality of the probability density function is that of the inversed-length. Hence, by definition, the numeric 1 in the numerator of Eqn 1 must have no unit and simply represent a *probability.* The parameter ϵ, in the denominator of the equation, on the other hand, must have the length dimensionality and simply represent a *length interval* on x' where $|\psi(x')|^2$ is non-zero and constant. From QM, the latter condition corresponds to a case that the particle has a definite momentum and hence has a *uniform probability* of being anywhere on that interval [3] . The length interval ϵ, therefore, could be interpreted as the uncertainty $\delta x'$ in the spatial coordinate of the particle on x'. The

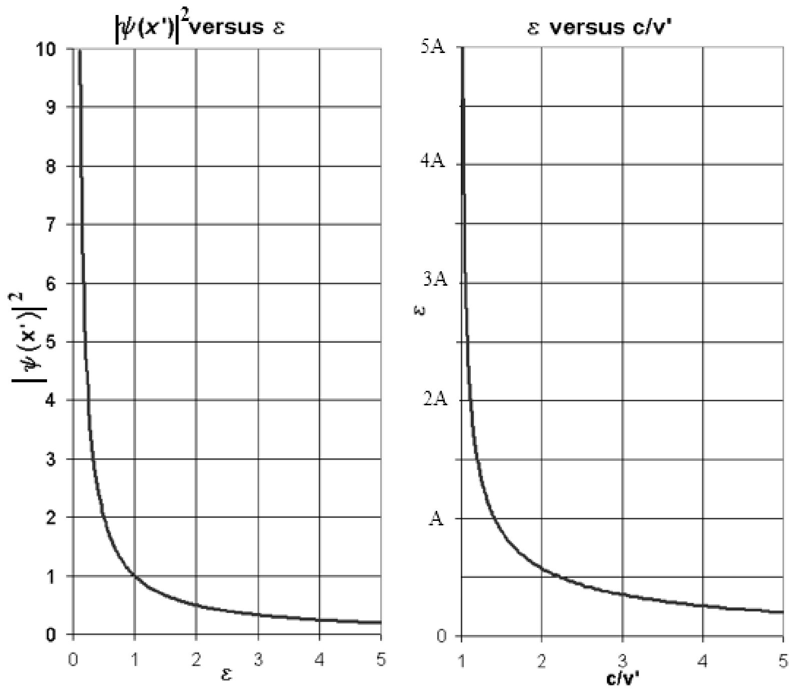

Figure 2: Probability density distribution $|\psi(x')|^2$ versus ϵ and ϵ versus c/v'

c-SRQM is based on a postulation that *the length interval corresponding to the spacetime coordinate uncertainty of a quantum particle obeys Lorentz transformation.* On that basis, it is postulated that the particle velocity v' and its spatial uncertainty ϵ along the path x' are related as follows:

$$\epsilon = \frac{A}{\sqrt{c^2/v'^2 - 1}} \tag{2}$$

[3]According to the revised definition of rest frame, the probability density distribution of a quantum particle in its nearest frame is expected to have a minimum length interval. In any other inertial frame of reference, the probability distribution covers a wider length interval compared to that of the nearest frame.

As will be shown later, the length interval A has two important features. First, it represents the *the invariant interval of the spacetime coordinate uncertainty four-vector in spacetime.* Second, it represents the *diameter of the event horizon of the smallest black hole in the universe.*

The functions $|\psi(x')|^2$ and ϵ, as defined in Eqn's 1 and 2, are shown in Fig 2. By examining Eqn 2, it clear that as the particle velocity $v' \to 0$, i.e. as it gets closer and closer to a stationary condition in I', the uncertainty in the position of the particle in that frame also approaches to zero, i.e. $\epsilon \to 0$, and subsequently, its spatial probability density distribution in that frame approaches to infinity, i.e. $|\psi(x')|^2 \to \infty$. Hence, *as expected for a stationary particle, the positional probability density distribution peaks where the particle is located and vanishes anywhere else on x'.* This is represented by the vertical axis in Fig 3a. Inversely, as the speed of the particle increases, the length interval ϵ, representing the uncertainty in spatial coordinate of the particle increases progressively in length, such that at the limit velocity $v' = c$, the spatial uncertainty becomes infinite, i.e. $\epsilon \to \infty$, and subsequently, $|\psi(x')|^2 \to 0$. This condition is shown by the horizontal axis in Fig 3a, representing a full uncertainty in the spacetime coordinate of a free photon prior to its observation by an inertial observer in I' . For all other conditions, where velocity of the particle is between two extreme limits, $0 < v' < c$, the spatial uncertainty ϵ and the magnitude of the wavefunction $|\psi(x')|^2$ assume some non-extreme values, as shown in Fig 3b. Finally, note that the area under the probability density distribution defined in Eqn (1) integrates to the probability of 1:

$$\int_{-\infty}^{\infty} |\psi(x')|^2 dx' \; = \int \frac{1}{\epsilon} dx' = 1 \tag{3}$$

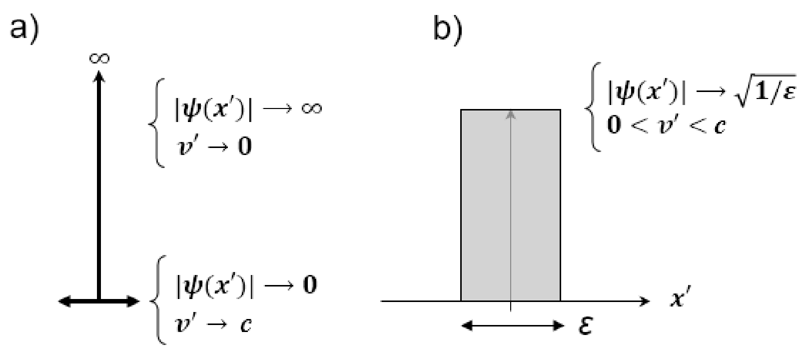

Figure 3: Spatial probability density distribution of a particle versus its velocity

3 Relativistic time dilation and quantum wavefunction

From Special Relativity, the intervals of proper-time $d\tau$ and coordinate-time dt' are related by the Lorentz transformation [1] as follows:

$$\frac{d\tau}{dt'} = \sqrt{1 - \frac{v'^2}{c^2}} \tag{4}$$

where the proper time τ is measured at the origin of the particle's nearest frame of reference I, and the coordinate time t' is measured at the origin of the inertial frame of reference I'.

The numerical value of the time dilation from Eqn 4, when v' is between two extreme cases of $v' = c$ and $v' = 0$ is always between 0 and 1, respectively. As the absolute probabilities associated with the uncertainty in the spacetime coordinate of a particle also vary between 0 and 1, it would not be surprising to show that the time dilations of SR and wavefunction of QM are physically related. To demonstrate this, we now re-arrange Eqn 4 as follows:

$$\frac{d\tau}{dt'} = \frac{v'}{c}\sqrt{\frac{c^2}{v'^2} - 1} \tag{5}$$

substituting for $\sqrt{c^2/v'^2 - 1}$ from Eqn 2 we get:

$$\frac{d\tau}{dt'} = \frac{v'}{c}\frac{A}{\epsilon} \tag{6}$$

and further by substituting for $1/\epsilon$ from Eqn 1 we arrive at a fundamental relationship between the *time dilation* of theory of Relativity and the *wavefunction* of Quantum Mechanics as follows:

$$\frac{d\tau}{dt'} = \frac{v'}{c}A|\psi(x')|^2 \tag{7}$$

Eqn 7, in a sense, relates *the relativistic time dilations corresponding to the kinematics of a particle with the probability density distribution of its position in space*. Multiplying both sides by c/v' and replacing $cd\tau = ds$, and $v'dt' = dx'$ we get:

$$A|\psi(x')|^2 dx' = ds \tag{8}$$

By integrating Eqn 8 over coordinate space x' we then arrive at:

$$A\int |\psi(x')|^2 dx' = \delta s \tag{9}$$

In reference to Eqn 3, the integral of Eqn 9 is equal to the probability of 1, therefore we finally arrive at the following relationship for the uncertainty interval invariant:

$$\delta s = A \tag{10}$$

and subsequently;

$$\delta\tau = \frac{A}{c} \tag{11}$$

Since both A and c are physical constants, the time interval A/c is considered to be the *cosmological time constant*, such that the age of universe can always be described by an integer multiple of the time constant - agreeable by all observers in the universe.

4 Four-vector of spacetime coordinate uncertainties

The components of the four-vector of the spacetime coordinate uncertainties are the $c\delta t'$ plus three spatial uncertainties $\delta x'$, $\delta y'$ and $\delta z'$. In this paper, however, without a loss in generality, we have limited our analysis to the situation in which the spatial axes of the inertial frames of reference I and I' are all parallel and their relative motion is along their x, x'-axes. As shown in Fig 4, the invariant base of the uncertainty triangle in this case is *always* A, the hypotenuse is $c\delta t'$ and perpendicular to the base is $\delta x'$. Therefore, the quantum uncertainties in spacetime coordinate of a particle constitute a *timelike four-vector* with invariant length of $\delta s = A$. For an observer that travels with the particle, the hypotenuse would be parallel to the base. For that case, the space-like uncertainty $\delta x' = 0$ (as the particle would look stationary to the observer), but the time-like uncertainty of the particle would be the *constant* $\delta t' = \delta\tau = A/c$.

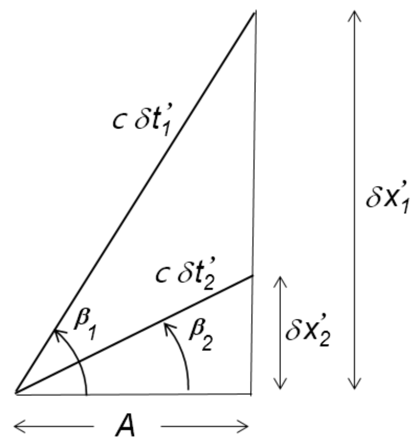

Figure 4: Invariant length A of uncertainty four vector of two particles with different velocities

5 The locus of uncertainties

Since the spacetime uncertainty interval $\delta s = A$ is invariant under the Lorentz transformation, it could be used to define the uncertainties $c\delta t'$ and $\delta x'$ in the spacetime coordinate of the particle as follows:

$$\delta s^2 = (c\delta t')^2 - (\delta x')^2 = A^2 \tag{12}$$

Eqn 12 represents a north-opening hyperbola as shown in Fig 5. The higher the coordinate

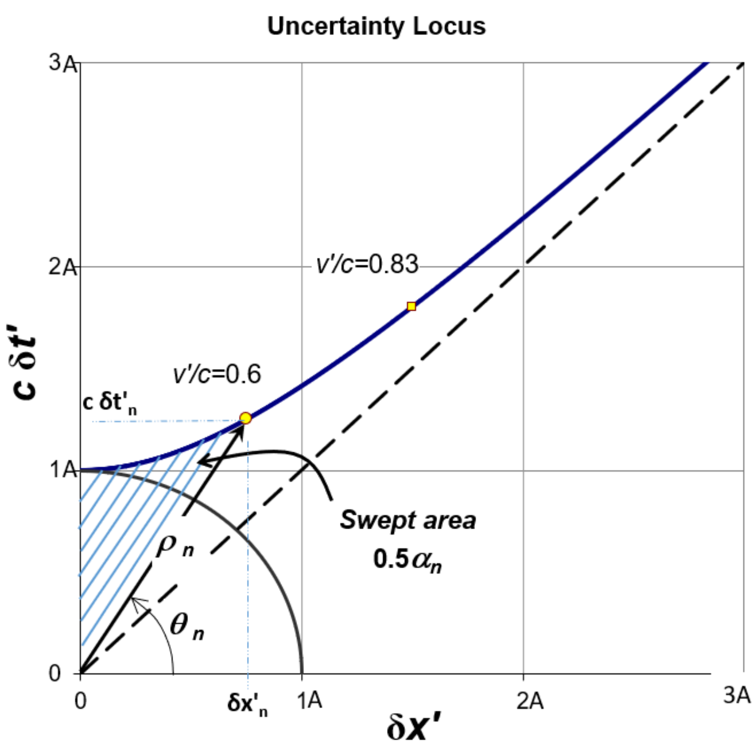

Figure 5: Locus of uncertainties of a particle in state of definite momentum

velocity v' relative to the inertial frame of reference I', the higher the uncertainty in the spacetime coordinates $c\delta t'$ and $\delta x'$ in that frame. Eqn 12 can be equivalently written as:

$$\cosh^2 \alpha - \sinh^2 \alpha = 1 \tag{13}$$

where the hyperbola parameter α is twice the area under the locus and the intersecting ray from the origin. In reference to Fig 5, for two particles with velocities of $v'/c = 0.6$ and $v'/c = 0.83$ for example, the difference in the spacetime uncertainties are $0.75A$ (space-like) and $0.55A$ (time-like).

The phase angle θ, represents the *instantaneous slope the world line* of the particle in spacetime and is given by:

$$\tan\theta = \frac{cdt'}{dx'} = \frac{c}{v'} \tag{14}$$

As shown in Fig 5, the phase angle θ varies between the limits $\pi/4 < \theta < \pi/2$, where the upper limit $\pi/2$ corresponds to the condition of a stationary particle where the vector ρ_n is closely (but not entirely) aligned with the time-like axis. As we shall see later, due to the quantum uncertainties, the phase angle θ of a stationary particle must always be less than $\pi/2$. The lower limit $\pi/4$ corresponds to that of the light particle where the vector ρ_n is closely (but again not entirely) aligned with the asymptote $\theta = \pi/4$.

Now it is worth to note that in Special Relativity the *light-like* (or null) interval has the invariant interval $c^2\delta t'^2 - \delta x'^2 = 0$, i.e $\theta = \pi/4$. In the combined SR-QM theory, however, the light-like signal is only *asymptotically* tangent to the line of 45 degree; hence, according to Eqn 12, the invariant interval in the case of a light particle is also $c^2\delta t'^2 - \delta x'^2 = A^2$, i.e. not zero.

The spacetime coordinate uncertainties, therefore, could be found by intersecting the uncertainty locus with the ray $c\delta t' = (c/v')\delta x'$ passing through the origin of the coordinate system. From Eqn 14, the slope of this intersecting ray is the instantaneous slope θ of the world line of the particle. Hence, the spacetime uncertainties $c\delta t'$ and $\delta x'$ can be obtained by solving the system of equations:

$$\begin{aligned} (c\delta t')^2 - (\delta x')^2 &= A^2 \\ c\delta t' - (c/v')\delta x' &= 0 \end{aligned} \tag{15}$$

which results in:

$$\begin{aligned} \delta x' &= \rho\cos(\theta) = A\sinh(\alpha) = \frac{Av'}{\sqrt{c^2 - v'^2}} \\ c\delta t' &= \rho\sin(\theta) = A\cosh(\alpha) = \frac{Ac}{\sqrt{c^2 - v'^2}} \end{aligned} \tag{16}$$

Using Eqn 16, we finally arrive at the following for the magnitude ρ :

$$\rho = A\sqrt{\frac{c^2 + v'^2}{c^2 - v'^2}} \tag{17}$$

From Eqn's 16 and 17 we then have:

$$\begin{aligned} \cos(\theta) &= \frac{v'}{\sqrt{c^2 + v'^2}} \\ \sin(\theta) &= \frac{c}{\sqrt{c^2 + v'^2}} \end{aligned} \tag{18}$$

where θ, as discussed before, is the slope of particle's world line. The relativistic equations developed in this section will be quantized in the following section.

6 Quantization of spatial uncertainties

Having $|\psi(x')|^2$ as defined in Eqn 1 in the previous section, we are now ready to write for the wavefunction of a particle under a definite momentum p as follows:

$$\psi(x') = \sqrt{\frac{1}{\epsilon}} e^{ipx'/\hbar} \tag{19}$$

where $\hbar = h/2\pi$ is the reduced Planck constant. Since the function $|\psi(x')|^2$ has to be single valued function on domain x', we demand for the periodicity of the wavefunction for *any* spatial uncertainty ϵ, i.e $\psi(x') = \psi(x' + \epsilon)$, hence:

$$\sqrt{\frac{1}{\epsilon}} e^{ipx'/\hbar} = \sqrt{\frac{1}{\epsilon}} e^{ipx'/\hbar} e^{ip\epsilon/\hbar} \tag{20}$$

From the last equation, we then have $e^{ip\epsilon/\hbar} = 1$, hence:

$$\frac{p_n \epsilon_n}{\hbar} = 2\pi n^2 \tag{21}$$

The reason for choosing a square of the quantum index n in the RHS is because each parameter in the product $p_n \epsilon_n$ in the LHS contributes one quantum index n. Isolating p_n in Eqn 21 we have:

$$p_n = \frac{h}{\epsilon_n} n^2 \tag{22}$$

From the theory of Special Relativity, however, for the momentum of the particle we have:

$$p = \frac{mv'}{\sqrt{1 - \frac{v'^2}{c^2}}} \tag{23}$$

multiplying both the numerator and denominator by c/v' we get:

$$p = \frac{mc}{\sqrt{\frac{c^2}{v'^2} - 1}} \tag{24}$$

substituting for $\sqrt{c^2/v'^2 - 1}$ by ϵ/A in the previous equation we get:

$$p_n = mc\frac{\epsilon_n}{A} \tag{25}$$

and now by substituting for p_n from Eqn 22 and solving for ϵ_n we get:

$${\epsilon_n}^2 = A\frac{h}{mc} n^2 \tag{26}$$

By definition, Compton wavelength [2] of a particle represents *the wavelength of a photon whose energy is equal to the rest energy of the particle*; therefore, for a particle with rest mass m we have:

$$mc^2 = \frac{hc}{\hat{\lambda}} \tag{27}$$

which in turn gives the following for the Compton wavelength of a particle with rest mass m:

$$\hat{\lambda} = \frac{h}{mc} \tag{28}$$

Now, let's define a *reference mass* $\bar{m}$ whose Compton wavelength $\hat{\lambda} = A$ as follows:

$$\bar{m} = \frac{h}{Ac} \tag{29}$$

Note that $\bar{m}$ represents *a particle whose rest mass is the smallest none-zero mass physically possible*; therefore, any particle with rest mass less than $\bar{m}$ is treated as a massless particle in the universe. Substituting for the term h/Ac in Eqn 26 from Eqn 29, gives an explicit equation for the spatial uncertainty ϵ_n in terms of particle mass m and reference mass $\bar{m}$ as follows:

$$\epsilon_n = A\sqrt{\frac{\bar{m}}{m}}\, n \qquad\qquad n = 1, 2, ... \tag{30}$$

Accordingly, *the spatial uncertainty of a particle is inversely proportional to square root of its rest mass* m. It is also evident that the minimum spatial uncertainty corresponds to that of a stationary particle with the minimum quantum index $n = 1$. The higher the quantum index n the higher the particle velocity and therefore the spatial uncertainty.

7 Quantization of momentum

The quantized form of momentum p_n, could simply obtained from Eqn 25 by substituting for ϵ_n from Eqn 30 as follows:

$$p_n = c\,\sqrt{m\bar{m}}\, n \qquad\qquad n = 1, 2, ... \tag{31}$$

According to Eqn 31 *the momentum of a particle is directly proportional to the square root of its rest mass* m.

8 Quantization of timelike uncertainties

The equation of the coordinate time uncertainty $\delta t'$ will be obtained from Eqn 12 by substituting for $\delta x'$ from Eqn 30 as follows:

$$\delta t'_n = \frac{A}{c}\sqrt{1 + \frac{\bar{m}}{m} n^2} \qquad\qquad n = 1, 2, ... \tag{32}$$

9 Quantization of particle velocity

The relativistic coordinate velocity v' can be obtained from Eqn 24 by substituting for momentum p from Eqn 31 and solving for c/v' as follows:

$$\frac{c}{v'_n} = \sqrt{1 + \frac{m}{\bar{m} n^2}} \qquad\qquad n = 1, 2, ... \tag{33}$$

From Eqn 33, the coordinate velocity of a particle with rest mass m at the quantum index $n = 1$ is given by:

$$v'_1 = c\sqrt{\frac{\bar{m}}{m + \bar{m}}} \tag{34}$$

Coordinate velocity v'_1 represents the particle velocity at its nearest frame of reference, i.e. it represents the *smallest* none-zero velocity that the particle could attain. From Eqn 34, it is evident that the higher the rest mass m of a particle the smaller is its near rest velocity. The near rest velocity of the reference mass $\bar{m}$ is then given by $\bar{v}'_1 = c/\sqrt{2}$.

10 Quantization of phase angle

The quantized equation of the phase angle θ could be obtained from Eqn 24 as follows:

$$\frac{c^2}{v'^2} = 1 + \frac{m^2c^2}{p^2} \tag{35}$$

substituting for c/v' and p from Eqn's 14 and 31, respectively, and solving for the phase angle θ we will have:

$$\theta_n = \tan^{-1}\sqrt{1 + \frac{m}{\bar{m}n^2}} \qquad n = 1, 2, ... \tag{36}$$

From Eqn 36, for a stationary particle with the quantum index $n = 1$, we have:

$$\theta_1 = \tan^{-1}\sqrt{1 + \frac{m}{\bar{m}}} \tag{37}$$

From above, for particle species of $m < \bar{m}$, as $m = 0$ physically, the term $\sqrt{1 + m/\bar{m}} = 1$ and with that $\theta_1 = \pi/4$. Hence, *the quantized equation of phase angle confirms that the massless particles with $m = 0$ travel with the speed of light.* Inversely, for particles of increasing larger mass, the term $\sqrt{1 + m/\bar{m}}$ increases boundlessly and with that the phase angle $\theta_1 \to \pi/2$, reducing the coordinate uncertainties at near rest condition. Therefore, *the higher the rest mass of a particle the less the spacetime coordinate uncertainties in its near rest condition.*

11 Quantization of energy

According to the theory of Special Relativity, the total energy E of a particle in terms of its mass m and momentum p is given by:

$$E^2 = p^2c^2 + m^2c^4 \tag{38}$$

substituting for the momentum p from Eqn 31, we then find particle's total energy in discrete values n as follows:

$$E_n = mc^2\sqrt{1 + \frac{\bar{m}}{m}n^2} \qquad n = 1, 2, ... \tag{39}$$

According to Eqn 39, the *relativistic rest energy $E = mc^2$* requires a correction for quantum particles for which the absolute rest condition is prohibited. Therefore, for the lowest quantum index $n = 1$ we have:

$$E_1 = mc^2\sqrt{1 + \frac{\bar{m}}{m}} \tag{40}$$

It is event that the quantum multiplier $\sqrt{1 + \bar{m}/m}$ in front of mc^2 is greater than one. As mentioned above, this is to account for the fact that in quantum mechanics, unlike relativity, the rest condition in its absolute sense is prohibited. Hence, *the total energy of a particle near rest is equal to its relativistic rest energy $E = mc^2$ augmented by the quantum rest kinetic energy.* Moreover, for particles of increasing larger mass, the term $\sqrt{1 + \bar{m}/m} \to 1$ and with that $E_1 \to mc^2$. This means *the kinetic energy corresponding to the rest condition of a massive particle is physically zero* - an axiom in the classical physics.

12 Upper limit of acceleration

In addition to the *four-vector of coordinate intervals* that obey Lorentz transformation and have an invariant interval, velocities and accelerations in the theory of relativity also constitute four-vectors. Derivative of the coordinate intervals with respect to the proper-time τ are called *proper-velocities*. They constitute a *time-like* four-vector with the invariant length c. Derivative of proper-velocities with respect to the proper-time generate a *space-like* four-vector of proper-accelerations. By definition, the invariant length of proper-acceleration four-vector is called local-acceleration a, which physically is understood to be the magnitude of the acceleration relative to an inertial frame which is instantaneously at rest with the accelerating particle. The limit local acceleration a_u is a direct consequence of the lower limit velocities v_1', upper limit velocity c and the uncertainty time interval $\delta t_1'$. The limit acceleration a_u corresponds to a case that the coordinate velocity of a particle, varies from the lower limit of the stationary value v_1', given by Eqn 34, to the upper limit c, within the invariant time interval $\delta\tau = A/c$. Hence,

$$a = \frac{c^2}{A}(1 - \sqrt{\frac{\bar{m}}{m + \bar{m}}}) \tag{41}$$

It is evident that for particles of large mass where $m \gg \bar{m}$ the term $\sqrt{\bar{m}/(m + \bar{m})} \to 0$ and with that the local acceleration $a \to a_u$ given by:

$$a_u = \frac{c^2}{A} \tag{42}$$

The latter represents the maximum acceleration a particle can attain in the physical world. More intuitive discussion on the limit acceleration can be found in [5]. In the following section, we discuss the consequences of applying the combined theory to the black holes.

13 Unit Black Hole

While it may seem counter intuitive, the gravitation pull at the event horizon of black holes reduce by the increase of their mass. For instance, doubling the mass of a black hole would reduce its gravitational pull at the event horizon by half. Therefore, it turns out that the physical limit of acceleration a_u, must correspond to the gravitational pull at the event horizon of the *least massive* black hole in nature, herein, named a Unit Black Hole (UBH). The physical limit of acceleration c^2/A can then be used to constrain the mass and size of UBH. The reason for such naming will become apparent when the quantization of the black holes mass, singularity, event horizon and temperature will be discussed at the subsequent sections. Accordingly, for the event horizon radius R_E of a black hole with mass M_B using Schwarzchild's equation [6] we have:

$$R_E = \frac{2GM_B}{c^2} \tag{43}$$

To arrive at the limit acceleration a_u, we now define UBH as a black hole whose event horizon diameter is A and mass M_1, and re-write the Schwarzchild Eqn 43 for the UBH as follows:

$$\frac{A}{2} = \frac{2GM_1}{\frac{c^2}{A}A} \tag{44}$$

substituting for c^2/A from Eqn 42 and re-arranging we arrive at:

$$a_u = \frac{GM_1}{(\frac{A}{2})^2} \tag{45}$$

From Eqn 45, we conclude that the limit acceleration a_u should be interpreted as the local acceleration of a free-falling particle when located at the distance $A/2$ from the geometric center of the UBH. At that distance, the gravitational pull is at limit and cannot physically increase any further. Re-arranging Eqn 45 further and substituting for a_u from Eqn 42 we then arrive at the mass of UBH as follows:

$$M_1 = \frac{Ac^2}{4G} \tag{46}$$

The mass M_1 and the diameter A represent the mass and size of the smallest black holes in the universe.

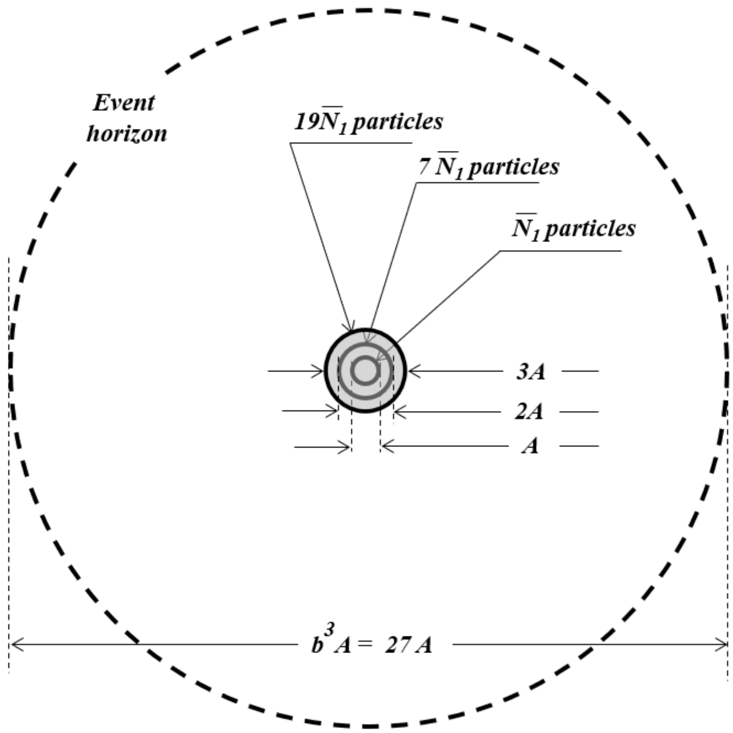

Figure 6: Event horizon and core of a b=3 black hole with the number of PSPs on each shell

14 Quantized black hole mass and size

Equipped with the system of equations developed under this theory, the quantization of basic black hole properties could now be done with different choices. One such choice, which was explored originally when the theory was first introduced in [3], was to let the diameter of event horizon D_b to increase by one Planck length L_p per quantum index b increase, ie $D_b = A + b\,L_p$. However, such a choice of quantization was shown not to produce a consistent description of the interior structure of black holes. A more useful quantization of the event horizon diameter D_b which offers a consistent description of the interior structure of black holes in terms of their constituents can be realized by the following:

$$D_b = b^3\,A \qquad\qquad b = 1, 2, ... \tag{47}$$

where as mentioned before b is the *quantum index of black holes*. It is clear that $b = 1$ gives $D_1 = A$, as expected for a stand alone UBH. Using Eqn 47, from Schwarzchild Eqn 43 we then have the following for the mass M_b of black holes:

$$M_b = b^3 \, M_1 \qquad\qquad b = 1, 2, ... \tag{48}$$

where M_1 is the mass of UBH as discussed before. With that the diameter of the physical singularity or the *core* C_b of black holes will be determined by:

$$C_b = (\frac{D_b}{A})^{1/3} \, A = b \, A \qquad\qquad b = 1, 2, ... \tag{49}$$

Comparing Eqn's 49 and 47, it is evident that the condition $C_b < D_b$ is true for all black holes more massive than UBH. This is as expected, since by the very definition of black holes, *the singularity is always engulfed by the event horizon.* Furthermore, for the UBH with $b = 1$, from Eqn 49 we then have $C_1 = D_1 = A$; meaning that the singularity and event horizon of the unit black hole *coincide* at diameter A, a feature uniquely valid for the UBH. As shown in Fig 6, the number of PSP particles $\bar{N}_b$ on a given shell b would then be given by:

$$\bar{N}_b = (3b^2 - 3b + 1)\bar{N}_1 \qquad\qquad b = 1, 2, ... \tag{50}$$

where $\bar{N}_1$ is the number of PSP constituents of quantum index $n = 1$ on the innermost UBH shell given by :

$$\bar{N}_1 = \frac{M_1}{\bar{m}} = \frac{A^2 c^3}{4Gh} = \frac{1}{4}(\frac{A}{L_p})^2 \tag{51}$$

Considering Eqn 51 we note that since *perfect squares of odd numbers are never divisible by* 4, the necessity of $\bar{N}_1 \in \mathbb{N}$ then demands that *the Planck length L_p must be an even divisor of UBH diameter A*, as shown in Fig 7. Also note that such arrangement of the particle

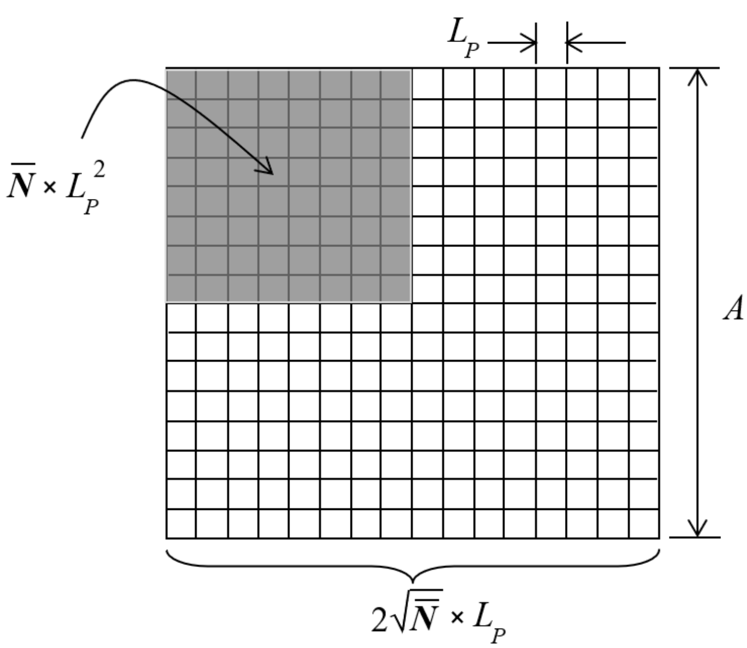

Figure 7: Planck length L_p must be an even divisor of UBH diameter A

count on the core shells makes the overall density ρ_s of all black hole singularities to be the constant:

$$\rho_s = \frac{3c^2}{2\pi G A^2} \tag{52}$$

An alternative cosmological model was proposed in [4], wherein the universe, prior to its expansion at the Big Bang, was assumed to be at a condensed state at the core of a mother primordial black hole (MPBH) of density ρ_s. Diametrically opposite to the standard cosmological model wherein the universe begins from *nothing*, in the alternative model, the universe begins from *everything*. In this model, the spherical shells of PSP condensation comprising the MPBH core were permitted to expand from the initial radial velocity of zero to the speed of light c within only one *cosmological time step* A/c. We also noted that the expansion of the core shells relative to their local rest frames under such rate would be consistent with the physical limit of acceleration c^2/A discussed earlier. The resulting model universe, which begins *decelerating* immediately after the Big Bang, was then shown to fit the observational data of the redshifts of distant supernovae rather well. In this model, dark energy was excluded in the analysis and only the visible and dark matter were taken into account. From the model, the known universe was shown to be the observable part of a much bigger structure, named as the *grand* universe. Moreover, it was shown that the model universe permits a cosmic microwave background (CMB) dipole whose *magnitude* is a function of the position of the observable universe within the grand universe. The *orientation* of the dipole in the sky was shown to be a function of the Milky way's orientation relative to the Hubble flow. In this model, the age of universe was found to be a few billion years older than that of the standard cosmological model. This, in turn, could explain the JWST observation of galaxies of very high redshifts whose structural maturity are found to be at odds with their *temporal* proximity to the big bang of the standard cosmological model, hence, offering them little time to acquire observed structural complexity. More importantly, the proposed model permits supermassive black holes to actually predate galaxies, as they are thought to be tiny remnants of the core of the MPBH which happened to randomly survive the expansion at big bang and remain condensed. The mechanism can also explain the source of *lone* black holes which have no significant stelar structure around them.

From the discussion above, it now may be somewhat clear why the name *primordial stem particle* was given to the particle of mass $\bar{m}$: *primordial* in a sense that the particle being the constituents of the MPBH predates the Big Bang, and *stem* in a sense that any form of matter that crosses the event horizon will ultimately transform to the primordial form prior to condensing *onto* the surface of singularity where an extreme gravity and temperatures near absolute zero is present. In other words, surrounding to a black hole singularity of index b are countless PSP's of quantum index $n > b$ from which $\bar{N}_{b+1}$ will eventually condense onto the singularity surface and generate shell $b+1$ followed by $\bar{N}_{b+2}$ particles to generate shell $b+2$ and so on. Therefore, the density of PSP is at the physical limit ρ_s at the singularity and reduces from the peak at the centre all the way to the edge of the host galaxy.

15 LIGO-Virgo GW constraint on UBH mass

In this section, we will make an attempt to constrain the UBH mass M_1 and its diameter A by utilizing the LIGO-Virgo observational gravitational wave (GW) data collected from a set of merger events of binary black holes (BBH). We then use the constraint on the UBH mass and size to arrive at the PSP mass $\bar{m}$. The basic numerical approach taken was to generate a fine Bayesian posterior grid on a range of possible values of M_1 and then find a set of quantum index pairs (p, q) that best fit the chirp mass $\mathcal{M}_c$ while satisfying the event black holes masses within the uncertainties of the LIGO data. In other words, the aim was to find the *most probable* common denominator M_1 such that in all events the triplet (p, q, M_1)

reproduces $\mathcal{M}_c$ and individual black holes within the given uncertainties. Figure 8 is the output of an AI-assisted code that was developed after several iterations for this aim. As

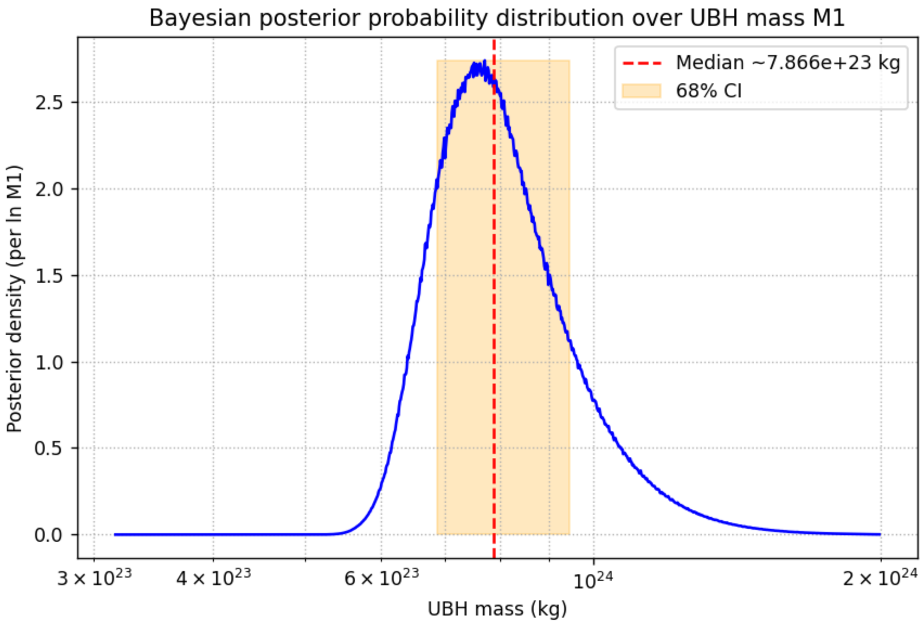

Figure 8: UBH mass M_1 estimated using GW data of 10 BBH merger events

summarized in Table 1, the code first reads the observed chirp mass $\mathcal{M}_{c,obs}$ and the binary black holes masses $m_{1,obs}$ and $m_{2,obs}$ plus their corresponding *asymmetric* uncertainties σ^+ and σ^- in each case. The observable chirp mass and binary black hole masses used in this analysis was taken from [7]. The code then scans over a given range of quantum index pairs

Event	Chirp mass M_c			Black hole mass m_1			Black hole mass m_2		
	σ-	median	σ+	σ-	median	σ+	σ-	median	σ+
GW150914	1.5	28.6	1.7	3.1	35.6	4.7	4.4	30.6	3.0
GW151012	1.2	15.2	2.1	5.5	23.2	14.9	4.8	13.6	4.1
GW151226	0.3	8.9	0.3	3.2	13.7	8.8	2.5	7.7	2.2
GW170104	1.8	21.4	2.2	5.6	30.8	7.3	4.6	20.0	4.9
GW170608	0.2	7.9	0.2	1.7	11.0	5.5	2.2	7.6	1.4
GW170729	4.8	35.4	6.5	10.2	50.2	16.2	10.1	34.0	9.1
GW170809	1.7	24.9	2.1	5.9	35.0	8.3	5.2	23.8	5.1
GW170814	1.1	24.1	1.4	3.0	30.6	5.6	4.0	25.2	2.8
GW170818	1.7	26.5	2.1	4.7	35.4	7.5	5.2	26.7	4.3
GW170823	3.6	29.2	4.6	6.7	39.5	11.2	7.8	29.0	6.7

Table 1: BBH masses and uncertainty levels used in the posterior analysis of UBH mass

(p, q) and a fine-grid of possible UBH mass M_1 and computes the resulting *fit* black hole masses $\hat{m}_1$ and $\hat{m}_2$:

$$\hat{m}_1 = p^3 \, M_1, \qquad \hat{m}_2 = q^3 \, M_1 \tag{53}$$

and *fit* chirp mass $\hat{\mathcal{M}}_c$ as follows:

$$\hat{\mathcal{M}}_c = \frac{(\hat{m}_1 \ \hat{m}_2)^{3/5}}{(\hat{m}_1 + \hat{m}_2)^{1/5}} \tag{54}$$

The *event likelihood* function $\mathcal{L}()$ then quantifies how well a candidate triplet (p, q, M_1) reproduces the observed values within their uncertainties σ^+ and σ^-. For each observable

X, ie. $\mathcal{M}_c$, m_1 and m_2 in each event, the log-likelihood contribution is based on a normal distribution:

$$\ln \mathcal{L}(X) = -\frac{1}{2}(\frac{\hat{X} - X_{obs}}{\sigma_X})^2 \tag{55}$$

where possibly asymmetric σ_X depends on whether the predicted $\hat{X}$ is above or below the measured observable X_{obs} as follows:

$$\sigma_X = \begin{cases} \sigma_X^- & \text{if } \hat{X} < X_{obs} \\ \sigma_X^+ & \text{otherwise} \end{cases} \tag{56}$$

The *total* log-likelihood to the event is then calculated using:

$$\ln \mathcal{L}_{event} = \ln \mathcal{L}(\mathcal{M}_c) + \ln \mathcal{L}(m_1) + \ln \mathcal{L}(m_2) \tag{57}$$

Finally, given Bayes' theorem, the posterior over parameters is given by:

$$P((p, q, M_1) \,|\, GW data) \propto \mathcal{L}_{event}(p, q, M_1) \;\times\; P(p, q, M_1) \tag{58}$$

where $P(p, q, M_1)$ is a prior uniformly defined over a range of binary index integers (p, q) and M_1. The range of these parameters are fine-tuned (by trial and error) to arrive at a unique feasible range that results in a meaningful probability distribution, as shown in Fig 8. The code then integrates (marginalize) the posterior, computes the median and the 68% CI, and reports the likelihood peak corresponding to the best-fit triplet (p, q, M_1) in the distribution. The source code for this analysis can be downloaded from Github as given Appendix A. Based on this analysis the Bayesian posterior probability over the UBH mass has the median $M_1 = 7.87 \times 10^{23}$ (kg) and 68% confidence interval of $[6.88 \times 10^{23} \,-\, 9.44 \times 10^{23}]$ (kg). This corresponds to $M_1 = 3.96 \times 10^{-7} M_{\odot}$, or maybe more conveniently, $M_1 = 10.071 M_{\otimes}$, where $M_{\odot} = 1.99 \times 10^{30}$ and $M_{\otimes} = 7.35 \times 10^{22}$ (kg) are the solar and lunar masses, respectively. The UBH event horizon has diameter with median of $A = 2.34$ (mm) and 68% confidence interval of $[2.04 \,-\, 2.80]$ (mm). Under these estimates, the PSP mass has median $\bar{m} = 9.55 \times 10^{-40}$ (kg), equivalent to 5.36×10^{-4} (eV). These results are summarized in Table 2.

	-1 σ	median	+1 σ	
UBH mass M_1	6.88E+23	7.87E+23	9.44E+23	(kg)
UBH diameter A	2.04	2.34	2.80	(mm)
PSP mass m_bar	1.08E-39	9.46E-40	7.89E-40	(kg)
N_1_bar	6.36E+62	8.32E+62	1.20E+63	(-)

Table 2: UBH mass M_1, diameter A, PSP mass $\bar{m}$ and particle count $\bar{N}_1$ on A

16 Explicit solution for triplet (p, q, M_1)

Now that an estimate for the most probable value of M_1 is obtained from the Bayesian Posterior approach, in this section we carry out a much finer search within the 68% CI neighborhood using an explicit approach. In this approach, the 68% confidence interval of $[6.88 \times 10^{23} \,-\, 9.44 \times 10^{23}]$ (kg) is divided to 10^6 substeps, and then the *lowest* M_1 in the interval which meets the condition $(p, q) \in \mathbb{N}$ while satisfying the observed frequency and chirp mass of the event is taken as the candidate for the UBH mass from that event.

		Original values	
Event	Probable UBH mass M1 (kg)	p	q
GW150914	7.340E+23	464	430
GW151012	7.045E+23	406	333
GW151226	6.998E+23	338	281
GW170104	7.040E+23	445	381
GW170608	7.034E+23	316	276
GW170729	7.046E+23	528	449
GW170809	8.962E+23	429	372
GW170814	7.403E+23	437	405
GW170818	6.977E+23	471	417
GW170823	8.178E+23	462	408
M1 Average (kg)	7.402E+23		
Standard Dev.	6.248E+22		
$M1_{\odot}$ (solar)	3.723E-07		
$M1_{☾}$ (lunar)	10.071		

Table 3: Probable UBH mass M_1 under each event using the explicit approach

		Revised		Original - Revised	
Event	Common UBH mass M1 (kg)	p	q	Δp	Δq
GW150914	7.402E+23	457	434	7	-4
GW151012	7.402E+23	396	331	10	2
GW151226	7.402E+23	332	274	6	7
GW170104	7.402E+23	435	377	10	4
GW170608	7.402E+23	309	273	7	3
GW170729	7.402E+23	512	450	16	-1
GW170809	7.402E+23	454	399	-25	-27
GW170814	7.402E+23	434	407	3	-2
GW170818	7.402E+23	456	415	15	2
GW170823	7.402E+23	473	427	-11	-19

Table 4: Common UBH mass M_1 among the events and the revised (p, q) indices

The results from the explicit approach is shown in Table 3 alongside with the explicitly obtained BBH indices (p, q) . The average M_1 from all the events is then taken as the most probable value for the UBH mass. The *average* of UBH mass from all ten events is found to be 7.402×10^{23} (kg) which is in line with the median of the Bayesian Posterior probability distribution over M_1. Moreover, the standard deviation of probable values of M_1 from the explicit approach is 6.59×10^{22} (kg), giving 68% CI of $6.74 \times 10^{23} - 8.06 \times 10^{23}$ (kg), again in line with what was obtained from Bayesian posterior probability distribution. Using the average M_1, this time common to all events, the BBH indices (p, q) were then revised (re-calculated). The differences between the explicitly obtained (p, q) indices and the revised ones are shown in Table 4. The resulting diameter of the physical singularity in each case is

Event	Singularity size (m)	
	m1	m2
GW150914	1.004	0.954
GW151012	0.870	0.727
GW151226	0.730	0.602
GW170104	0.956	0.828
GW170608	0.679	0.600
GW170729	1.125	0.989
GW170809	0.998	0.877
GW170814	0.954	0.894
GW170818	1.002	0.912
GW170823	1.039	0.938

Table 5: Diameter of the physical singularities in each BBH merger event

given in Table 5, and the resulting difference between the model and observed chirp masses and frequencies in each event is given in Table 6. Applying the theory to the Sagittarius A*

Event	Measured				Model				Δ (Measured - Model)			
	m1	m2	Chirp Mc	freq_s	m1	m2	Chirp Mc	freq_s	m1	m2	Chirp Mc	freq_s
GW150914	35.6	30.6	28.6	66.4	35.5	30.4	28.6	66.7	0.1	0.2	0.0	-0.3
GW151012	23.2	13.6	15.2	119.5	23.1	13.5	15.3	120.2	0.1	0.1	-0.1	-0.7
GW151226	13.7	7.7	8.9	205.5	13.6	7.7	8.8	206.8	0.1	0.0	0.1	-1.3
GW170104	30.8	20	21.4	86.6	30.6	20.0	21.4	87.0	0.2	0.0	0.0	-0.4
GW170608	11	7.6	7.9	236.4	11.0	7.6	7.9	237.1	0.0	0.0	0.0	-0.7
GW170729	50.2	34	35.4	52.2	50.0	33.9	35.7	52.5	0.2	0.1	-0.3	-0.3
GW170809	35	23.8	24.9	74.8	34.8	23.7	24.9	75.2	0.2	0.1	0.0	-0.4
GW170814	30.6	25.2	24.1	78.8	30.4	25.1	24.0	79.2	0.2	0.1	0.1	-0.4
GW170818	35.4	26.7	26.5	70.8	35.3	26.6	26.6	71.1	0.1	0.1	-0.1	-0.3
GW170823	39.5	29	29.2	64.2	39.4	29.0	29.4	64.4	0.1	0.0	-0.2	-0.2

Table 6: Discrepancy in chirp mass and frequency between the model and LIGO data

with $M_{sag} = 4.3 \times 10^6 M_\odot$, we have its index $b = (M_{sag}/M_1)^{1/3} \sim 22603$ and diameter of its singularity as $C_{sag} \sim 49.7$ (m). Details of the explicit solution for (p, q, M_1) can be found in Appendix B. The script used to generate the explicit results discussed in this section can be downloaded from Github as given in Appendix A.

17 Quantized Hawking temperature

Black holes temperature from Hawking's equation is given by [8]:

$$T = \frac{\hbar c^3}{8\pi G M \kappa} \tag{59}$$

where κ is the Boltzmann constant. Substituting for the black hole mass $M_b = Ac^2b^3/4G$ from Eqn 48 in Eqn 59 then the temperature of black holes in the quantized form will be as follows:

$$T_b = \frac{L_p}{D_b} T_p \tag{60}$$

where $T_p = m_p c^2/\kappa$ is the Planck Temperature. From above, UBH has the highest temperature $T_1 = T_p L_p / A$ among the black holes.

18 Interpretation of uncertainties

While the spacetime coordinate uncertainties $(\delta x', c\delta t')$ encountered in the c-SRQM theory do comply with the Heisenberg uncertainty principle, as was shown in [3], nonetheless, they should not be interpreted as identical to those of Quantum Mechanics. The c-SRQM uncertainties appear to be *inherent* to the physical reality, and in particular to the way *information* is propagating in the physical world. For instance, as discussed in [5], the local acceleration of an object along a given direction is proportional to the rate of change of its spatial uncertainty in that direction. As a consequence, acceleration of a particle by a rate exceeding the upper limit a_u would mean that the information on its likely whereabouts along the path needs to propagate superluminally - something not permitted physically.

19 Conclusion

Using results from the combined theory of special relativity and quantum mechanics, a quantum model for black holes singularity is proposed which is made of a set of concentric spherical shells. Quantum index of a black hole corresponds to the number of spherical shells in its singularity. Quantum index of black holes increases by the increase of their mass. The smallest black hole possible in the universe with quantum index one is consisted of a single shell whose diameter is a physical constant. The step size between any two successive shell in the singularity is equal to the diameter of the innermost shell. Each shell is shown to host a fixed number of constituents. The number of constituents on a shell is a function of the shell number and increases progressively towards the outer layers. Black holes singularity is thought to be condensation of a stem primordial particle whose rest mass is the physical limit for massless particles. The first shell is made of the condensation of a set of particles that are at the lowest possible quantum state, one. The second shell is made of the condensation of a larger set of particles that are at the second quantum state, two and so on. Entropy of black holes stem from the number of configurations that the comprising particles can arrange themselves on the shells. Any ordinary matter that falls into a black hole is transformed to the primordial form when exposed to the immense gravitation pull of the singularity and extreme cold temperatures. The primordial particles at quantum states higher than that of the outermost shell surround the singularity, and will condense only when a shell of lower quantum index is fully occupied by matching particles. Not only the internal space between the singularity and event horizon is filled with the primordial particles of higher quantum state, but these particles are thought to permeate the entire universe as relics from Big Bang. Having their density reaching to the peak value at the singularity, and gradually diminishing as distance increases, the particle could act as the backbone of dark matter. A set of gravitational wave observations attributed to binary black hole mergers by LIGO-Virgo systems were used to constrain the mass of the unit black hole.

References

[1] F. W. Sears and R. W. Brehme, 'Introduction to the theory of relativity', Addison-Wesley publishing company, 1968, p103

[2] A. H. Compton, 'A quantum theory of the scattering of x-rays by light elements', 1923, Physical Review, 21 (5):483-520

[3] F. Abrari, 'Combined theory of Special Relativity and Quantum Mechanics', https://viXra.org/abs/2106.0167

[4] F. Abrari, 'Cosmology of inevitable flat space', https://viXra.org/abs/2207.0028

[5] F. Abrari, 'On the quantum description of inertia', https://viXra.org/abs/2401.0138

[6] K. Schwarzchild, 'Uber das gravitationsfeld eines massenpunktes nach der Einsteinschen theorie', 1916, Sitzunggsberichte der deutschen akademie der wissenschaften zu Berlin, pp 189

[7] P.B. Abbott et al, 'GWTC-1: A gravitational-Wave transient catalog of compact binary mergers observed by LIGO and Virgo during the first and second observing runs', Physical Review X 9, 03m1040, (2019)

[8] B. J. Carr, 'Primordial Black Holes - Recent Developments', 22nd Texas Symposium, Stanford, 12-17 Dec 2004, arXiv:astro-ph/0505034v1 1 Apr 2005

A Appendix A - the AI-assisted source codes

The source codes for the Bayesian posterior probability approach and the explicit search around its median can be found in :
`https://github.com/FaridAbrari/UBH-mass`.
Source codes: LIGO_GITHUB.v8.py & Explicit.GITHUB.v5.py

B Appendix B - Explicit solution for (p, q)

In this section we describe an AI-assisted explicit solution. The approach is used to determine the triplet (p, q, M_1) which satisfies the observed chirp mass $\mathcal{M}_c$ and f_c of its corresponding BBH merger event. Assume the masses m_1 and m_2 of a BBH merger event could be described by:

$$\begin{aligned} m_1 &= x \times M_1 \\ m_2 &= y \times M_1 \end{aligned} \tag{B.1}$$

where as before M_1 is the UBH mass and the multipliers (x, y), as required by the theory, are perfect cubes:

$$\begin{aligned} x &= p^3 \\ y &= q^3 \end{aligned} \tag{B.2}$$

meeting the requirement $(p, q) \in \mathbb{N}$ for each merger event. First define new variables *sum* S and *product* P of the multipliers x and y such that:

$$\begin{aligned} S &= x + y = p^3 + q^3 \\ P &= x \times y = (p \times q)^3 \end{aligned} \tag{B.3}$$

Then define coefficient $\mathcal{F}_\chi$ in the chirp mass Eqn 54 such that:

$$\mathcal{M}_c = \mathcal{F}_\chi\, M_1 \tag{B.4}$$

we therefore have the coefficient $\mathcal{F}_\chi$ in terms of S and P as follows:

$$\mathcal{F}_\chi = (\frac{P^3}{S})^{1/5}. \tag{B.5}$$

From ISCO-style mapping for a characteristic frequency, a simple approximation for the GW wave frequency scale (source-frame) is:

$$f_c \approx \frac{c^3}{6^{3/2} \pi G M_{total}} \tag{B.6}$$

Knowing $M_{total} = (x + y)M_1 = SM_1$ we then have:

$$S = \frac{B}{M_1} \tag{B.7}$$

where the constant B of each merger event is obtained by knowing the observed f_c from:

$$B = \frac{c^3}{6^{3/2}\pi G f_c} \tag{B.8}$$

Now substituting for S in $\mathcal{F}_\chi$ from Eqn B.7, and then substituting for the latter from Eqn B.5 in Eqn B.4 and solving for P we have:

$$P = \frac{K^{1/3}}{M_1^2} \tag{B.9}$$

where K is another constant obtained for each merger by knowing the observed $\mathcal{M}_c$ from:

$$K = B\,\mathcal{M}_c^5 \tag{B.10}$$

So using Eqn's B.7 and B.9 we have closed form expressions for the sum S and product P of the multipliers (x, y) in terms of UBH mass M_1 and observables f_c and $\mathcal{M}_c$. Now define summation U and product V of quantum indices p and q as follows:

$$\begin{aligned} U &= u + v \\ V &= u \times v \end{aligned} \tag{B.11}$$

where $u = p$ and $v = q$. Using the identity:

$$u^3 + v^3 = (u+v)^3 - 3uv\,(u+v) \tag{B.12}$$

we then have:

$$U^3 - 3VU - S = 0 \tag{B.13}$$

Note that since $V = uv = P^{1/3}$, for the coefficient V from Eqn B.9 we have:

$$V = \frac{K^{1/9}}{M_1^{2/3}} \tag{B.14}$$

Finally, by substituting for S and V from Eqn's B.7 and B.14 in Eqn B.13 we arrive at:

$$U^3 - 3\,(\frac{K^{1/9}}{M_1^{2/3}})\,U - \frac{B}{M_1} = 0 \tag{B.15}$$

From equation above if a real U exists then it can be used to recover (u, v) as the roots of the following quadratic:

$$t^2 - Ut + V = 0 \tag{B.16}$$

therefore:

$$(u, v) = \frac{U \pm \sqrt{U^2 - 4V}}{2} \tag{B.17}$$

Those values of M_1 that satisfy $(u, v) = (p, q) \in \mathbb{N}$ are considered *possible* candidates for the mass of UBH from that BBH merger event. At the end, let's remark that:

$$\begin{aligned} (t-u)(t-v) &= 0 \\ t^2 - vt - ut + uv &= 0 \\ t^2 - (u+v)t + uv &= 0 \\ t^2 - Ut + V &= 0 \end{aligned} \tag{B.18}$$

hence, the roots of the quadratic equation do indeed return $(u, v) = (p, q)$.